RESISTIVE EFFECTS IN THIN ELECTROCHEMICAL CELLS: DIGITAL SIMULATIONS OF CURRENT AND POTENTIAL STEPS IN THIN LAYER ELECTROCHEMICAL CELLS

IRA B. GOLDBERG* and ALLEN J. BARD

Department of Chemistry, University of Texas, Austin, Texas 78712 (U.S.A.)

(Received 6th December 1971; in revised form 9th February 1972)

INTRODUCTION

Electrochemical cells which exhibit high resistances and non-uniform current distributions include thin layer electrochemical cells[1], thin layer spectroelectro-chemical cells[2], cells with porous electrodes[3], and *in-situ* electrochemical electron spin resonance (e.s.r.) cells[4,5]. Two kinds of resistive effects are observed with these cells. The resistance between the working electrode and the reference electrode, or the uncompensated resistance, R_u, causes the actual potential at the working electrode to be different from the measured potential by an amount iR_u where i is the current. The second resistive effect is caused by the differences in solution resistance between different points on the working electrode and the auxiliary electrode. This causes different iR drops at different points on the working electrode, resulting in differences in potentials adjacent to the electrode surface and, therefore, non-uniform current distributions.

Generally, the theoretical treatments of electrochemical techniques do not consider non-uniform current densities because in most cases it is difficult to calculate these in closed form. Newman[6a] and Harrar and Shain[6b], however, have carried out several calculations which represent situations where resistive effects cause significant non-uniform current densities and deviate from the usual theoretical treatments. The technique of digital simulations[7-9] of electrochemical processes has been applied to a variety of electrochemical experiments. Recently Goldberg *et al.*[5] have used this technique to calculate the effect of solution resistance upon the e.s.r. signal in conventional *in-situ* electrochemical-electron spin resonance cells. The effect of solution resistance on potential steps and current steps in thin layer electrochemical cells is reported here.

DIGITAL SIMULATION

Simulations of electrochemical processes are discussed in detail by Feldberg[7]. The incorporation of the resistance in solution as well as finite diffusion into these calculations has also been described[5], and will not be repeated here. A schematic representation of the electrochemical cell is shown in Fig. 1. The resistance between

* Present address: North American Rockwell Science Center, Thousand Oaks, Calif. 91360, U.S.A.
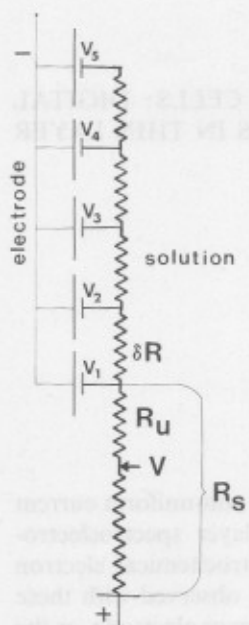
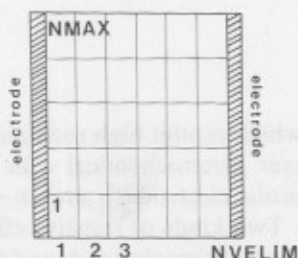Fig. 1. Schematic representation of a thin layer electrochemical cell.

Fig. 2. Digital representation of parallel plate thin layer electrochemical cell.

the counter electrode and the edge of the working electrode is designated R_s, and the uncompensated resistance as R_u. It is assumed in all cases that the resistance across the double layer is negligible and that the charge transfer is nernstian. The potential difference between the working electrode and the reference electrode is V. The potential at each segment k of the working electrode *vs.* the reference electrode is V_k (which represents the potential of the center of the electrode segment), and the current flowing into each segment is δi_k so that the total current I is:

$$I = \sum_{k=1}^{NMAX} \delta i_k \tag{1}$$

where NMAX is the number of segments of the working electrode. The representation of the parallel plate thin layer cell is shown in Fig. 2. The length of the segment of the electrode depends only on the precision desired in the calculation. In many cases the length of the electrode segment may be selected so that diffusion parallel to the electrode may be considered negligible compared to the diffusion perpendicular to the electrode, although, if greater accuracy is desired, the lateral diffusion may be included in the calculation.

Since the current of the kth electrode segment, δi_k, depends upon the potential at that element, V_k, and the potentials between elements are related by the iR drop, so that

$$V_{k+1} = V_k - \delta i_k R \tag{2}$$

the potential at some point at the electrode must be known before the potentials and

currents at each electrode segment can be calculated. The bisection method[10] of iteration was used to compute the currents and potentials. Slightly different procedures were used for constant current and constant potential experiments.

For simulations of constant current experiments, the sum of δi_k must satisfy eqn. (1) where i is equal to the current in the experiment. Note also that V_1 differs from V by the amount iR_u. In this method positive and negative limits of V, denoted V_{max} and V_{min}, are guessed. The first trial value of V is taken as $\frac{1}{2}(V_{max} + V_{min})$, V_1 is calculated and values of δi_k and V_k are calculated for all segments of the electrode. The total current, via eqn. (1) is then determined. If this current is too large, V_{min} is replaced by V, or if the current is too small, V_{max} is replaced by V, and the calculations are repeated until the desired degree of convergence is obtained. A flow chart of this program is shown in Fig. 3. Since relatively large currents are calculated here, it is not necessary to use double precision as in some cases computed for studies of e.s.r.-electrochemical cells[5].
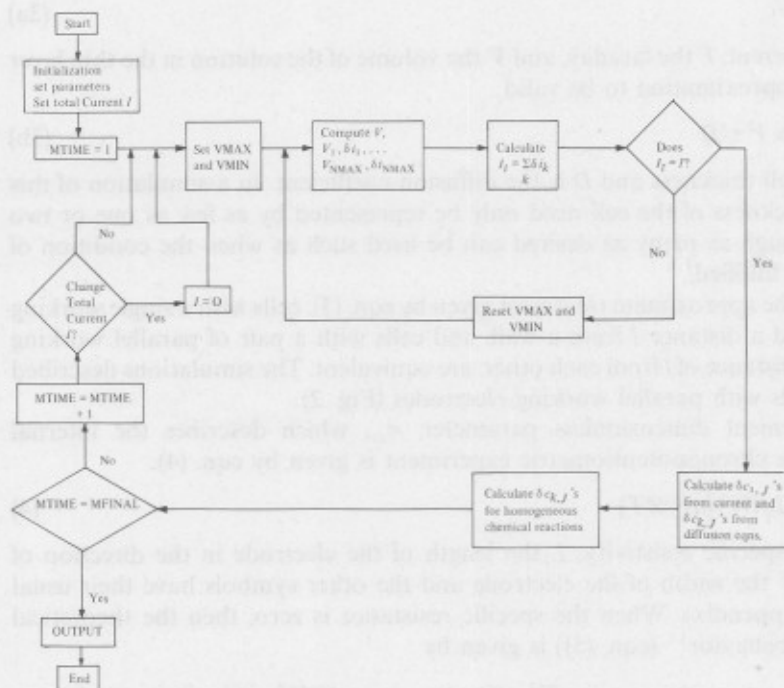

Fig. 3. Flow chart of digital simulation program.

For simulations of potential step experiments the current is not known. Thus, it is easier to guess V_{max} and V_{min} for the potential of V_{NMAX} (the potential of the electrode segment farthest from the counter electrode). As before, the potentials and currents for each of the electrode segments can be calculated by repeated application of eqn. (2). After V_1 and the total current are calculated, the value of $V_1 + R_u \sum_k \delta i_k$ may be compared to the applied potential. If the calculated potential is too negative, V_{min} is replaced by V_{NMAX}, or if it is too positive, V_{max} is replaced by V_{NMAX}. Convergence in this calculation is very rapid.

RESULTS

Simulations of chronopotentiometric experiments

Chronopotentiometry in thin layer electrochemical cells has been described in detail by Christiansen and Anson[11], and by Hubbard and Anson[1]. In their treatments, the effect of solution resistance was neglected because the current passing through the cell was restricted to extremely small magnitudes. Typically, currents of less than 500 μA cm^{-2} were used with resulting transition times (τ) usually greater than about 10 s. At higher current densities, the chronopotentiogram may become too ill-defined[11] to permit unambiguous measurement of τ.

If the current is sufficiently small, then the concentration of electroactive material during the experiment may be assumed uniform throughout the solution[1]. If this is indeed the case, then for a one-electron process in the absence of double layer charging and background currents

$$i\tau \sim nFVc \tag{3a}$$

where i is the current, F the faraday, and V the volume of the solution in the thin layer cell. For this approximation to be valid

$$nFVc/i \gg l^2\tau/D \tag{3b}$$

where l is the cell thickness and D is the diffusion coefficient. In a simulation of this process, the thickness of the cell need only be represented by as few as one or two segments, although as many as desired can be used such as when the condition of eqn. (3b) is not fulfilled.

Within the approximate treatment given by eqn. (3), cells with a single working electrode spaced a distance l from a wall, and cells with a pair of parallel working electrodes at a distance of l from each other, are equivalent. The simulations described here are for cells with parallel working electrodes (Fig. 2).

A convenient dimensionless parameter, σ_{cs}, which describes the internal resistance in the chronopotentiometric experiment is given by eqn. (4).

$$\sigma_{cs} = (\rho iL/lW)(nF/\mathscr{R}T) \tag{4}$$

where ρ is the specific resistivity, L the length of the electrode in the direction of current flow, W the width of the electrode and the other symbols have their usual meaning (see Appendix). When the specific resistance is zero, then the theoretical potential–time behavior[11] (eqn. (5)) is given by

$$E = E' + \frac{\mathscr{R}T}{nF}\ln\left\{\frac{\tau - t + \dfrac{2l^2}{\pi^2 D}\displaystyle\sum_{i=1}^{\infty}\frac{1}{K^2}\exp-\left(\dfrac{DK^2\pi^2 t}{l^2}\right)}{t + \dfrac{l^2}{3D} - \dfrac{2l^2}{\pi^2 D}\displaystyle\sum_{K=1}^{\infty}\frac{1}{K^2}\exp-\left(\dfrac{DK^2\pi^2 t}{l^2}\right)}\right\} \tag{5}$$

At times where $t \gg l^2/3D$ and $t - \tau \gg l^2/3D$, eqn. (5) becomes

$$E = E_{\tau/2} + (\mathscr{R}T/nF)\ln\left[(\tau - t)/t\right] \tag{6}$$

Several simulated chronopotentiograms for a one-electron transfer ($n = 1$) at different values of σ_{cs} are shown in Fig. 4. For these calculations, $l^2/3D\tau$ is approximately
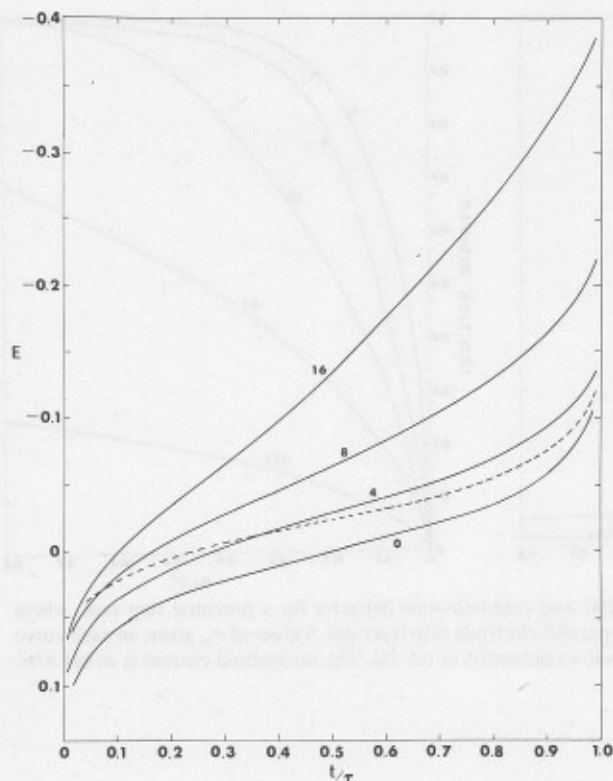
Fig. 4. Digital simulation of chronopotentiometry in parallel plate thin layer cells: $l^2/3D\tau = 0.02$. Values for parameter, σ_{cs}, given on each curve. Dotted line represents chronopotentiometry under conditions of semi-infinite linear diffusion.

0.0212, and cell parameters which would fit this calculation are $l = 30\ \mu m$, $L = W = 1.00$ cm, $i = 20\ \mu A$, $c = 10^{-3}\ M$, $D = 10^{-5}\ cm^2\ s^{-1}$. Based on these parameters the corresponding specific resistivities for the curves would be: for $\sigma_{cs} = 4.00$, $\rho = 15.4\ \Omega cm$; for $\sigma_{cs} = 8.00$, ρ 30.8 Ωcm; for $\sigma_{cs} = 16.0$, $\rho = 61.7\ \Omega cm$.

Furthermore, the reference electrode was assumed to be placed at a position where the uncompensated resistance is equal to the resistance between "adjacent" segments of the electrode. Since the current during the experiment is constant, the uncompensated iR does not affect the shape of the chronopotentiograms, but only changes its displacement along the potential axis.

Note from Fig. 4 that as the specific resistivity of the electrolyte increases, the measured value of $E_{\tau/2}$ becomes more negative, and the slope of the E vs. t curve increases, making the endpoint less well defined. At sufficiently high resistances, the potential at the leading edge of the electrode can become high enough that secondary electrochemical processes begin before the concentration of unreduced species becomes zero along the entire electrode surface[5]. As the approximation given in eqn. (3) becomes less valid, the shape of the chronopotentiogram also changes and approaches that obtained under conditions of semi-infinite linear diffusion (dotted line in Fig. 4).
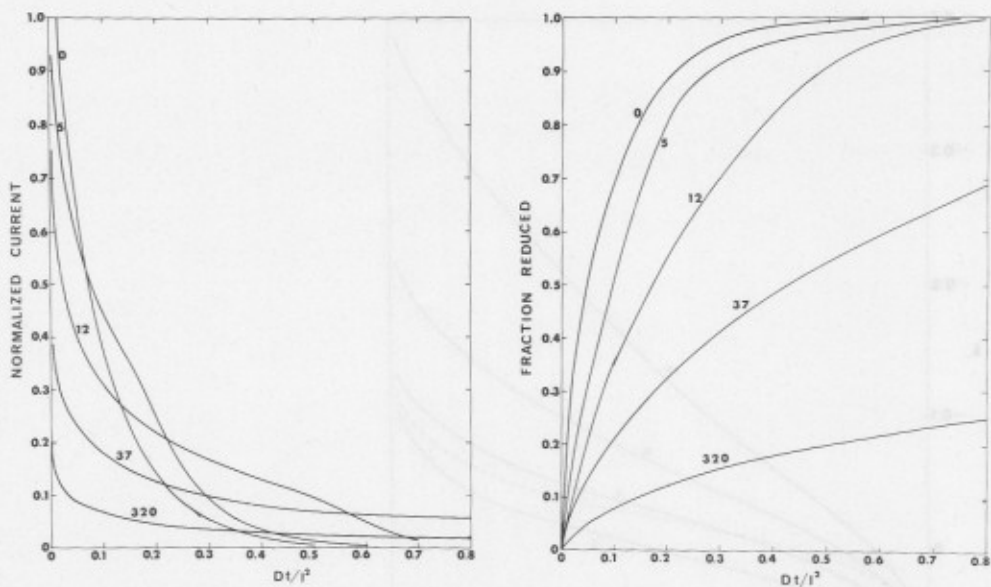
Fig. 5. Digital simulation of current–time and coulomb–time behavior for a potential step expt. where E (applied) $= E_{\frac{1}{2}} - 0.24$ V and $n = 1$ in a parallel electrode thin layer cell. Values of σ_{ps} given on each curve ($\sigma_{ps} = 0$ corresponds to the theoretical values presented in ref. 1a). The normalized current is $il/4nFADc$.
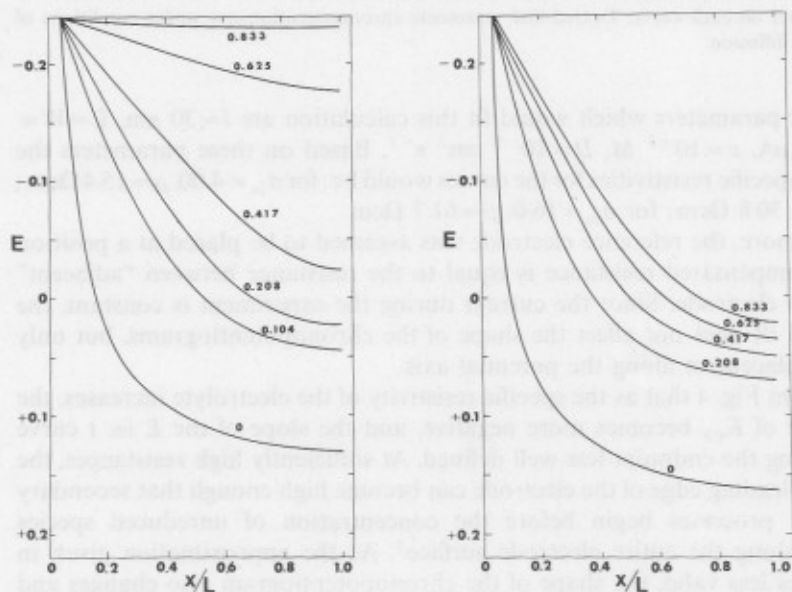

Fig. 6. Digital simulation of potential $vs.$ length at various times (DT/l^2) during a potential step expt. Right, $\sigma_{ps} = 37.4$; left, $\sigma_{ps} = 12.0$; $E = E_{\frac{1}{2}} - 0.24$ V.

Potential step experiments

Potential steps are not usually carried out in conventional thin layer cells because generally the initial currents are so high that extremely large iR drops occur. The advantage of potential steps in thin layer cells, however, is that the electrolysis will reach completion in a very short time ($l^2 t/D \sim 1$ for the parallel plate cell).

Although simulations of potential step experiments in both parallel and single electrode cells have been carried out, we will be concerned here only with the parallel plate system[1]. In these calculations the uncompensated resistance was assumed to be zero because under this condition the effects of potential gradients at the electrode surface are easier to examine independently. Uncompensated resistance effects can be added to the simulation without difficulty. Because the time of a potential step experiment is of the order of the value of l^2/D, the concentration gradients are significant, and the concentration must not be assumed uniform. Generally, more than 8 increments of cell thickness are required to simulate the potential step experiments.

A convenient parameter which describes the effect of electrolyte resistance is given by eqn. (7)

$$\sigma_{ps} = \rho \left(n^2 F^2 / \mathscr{R} T \right) Dc \left(L/l \right)^2 \tag{7}$$

$nF/\mathscr{R}T$ merely converts current and voltage to the appropriate parameters. Since the current is proportional to D and c, the diffusion coefficient and the concentration
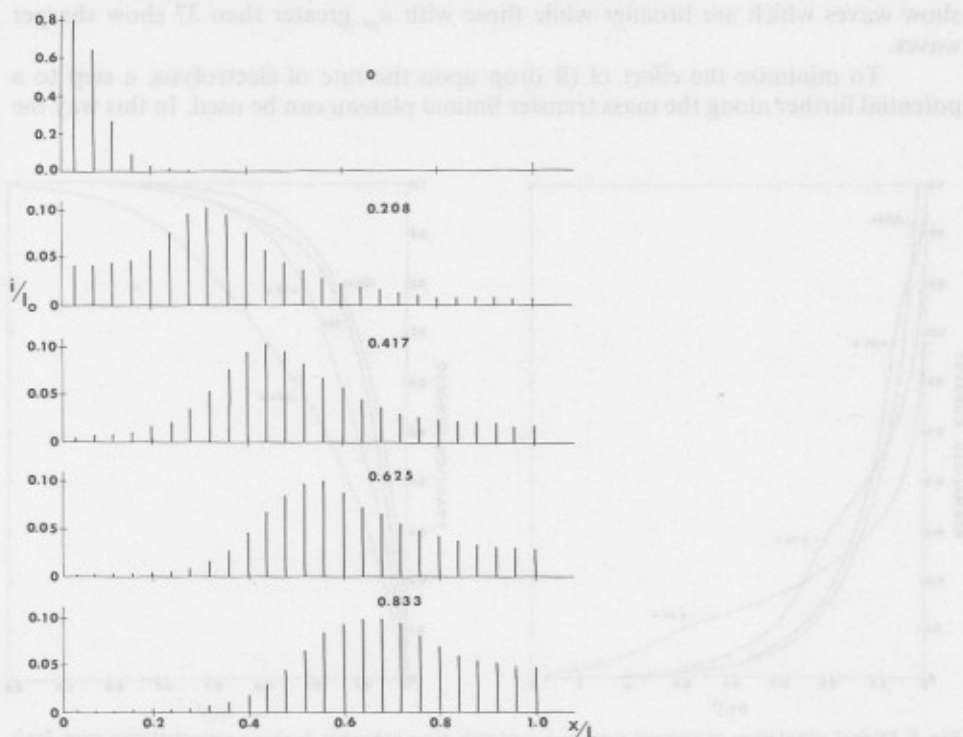

Fig. 7. Digital simulation of fraction of current at different segments of the working electrodes at various times during a potential step expt., $\sigma_{ps} = 37.4$. Bar represents current at center of each electrode segment.

respectively, the voltage drop along the electrode will be proportional to these values. However, L and l appear to the second power because of the dependence of both i and R on these parameters (see Appendix).

The simulations have been carried out in a dimensionless form, but it is more illustrative to relate the parameters to a real system. The characteristics of the cell described here could be as follows: $L = W = 1$ cm, $l = 30$ μm, $c = 10^{-3}$ M, and $D = 10^{-5}$ cm^2 s^{-1}. Based on these values, a σ_{ps} of 12.30, 37 and 320 would correspond approximately to the following electrolytes: aqueous 1 M HClO$_4$, 1 M KCl, and 0.1 M KCl. A one-electron reduction and a soluble reactant (O) and product (R) are assumed. Figure 5 shows the calculated current–time and coulomb–time behavior in a parallel electrode thin layer cell where the applied potential is 0.24 V more negative than the half-wave potential of the redox couple (taken as equal to 0) and only O is initially present. The resistance effect with even very strong electrolytes is marked. The potential distribution across the working electrode at different times during the potential step is shown in Fig. 6. In the absence of resistive effects, the whole electrode would be maintained at the applied potential (-0.24 V). However because of iR drops, only the edge of the electrode adjacent to the reference electrode is actually maintained at that value. The gradient is a function of the electrolyte resistance. The relative current densities at the electrode are shown in Fig. 7 for the system in which $\sigma_{ps} = 37.4$. Because the current decreases continually during the experiment (see Fig. 5), the wave of current moves farther along the electrode. Similar diagrams for σ_{ps} less than 37 show waves which are broader while those with σ_{ps} greater than 37 show sharper waves.

To minimize the effect of iR drop upon the rate of electrolysis, a step to a potential further along the mass transfer limited plateau can be used. In this way the
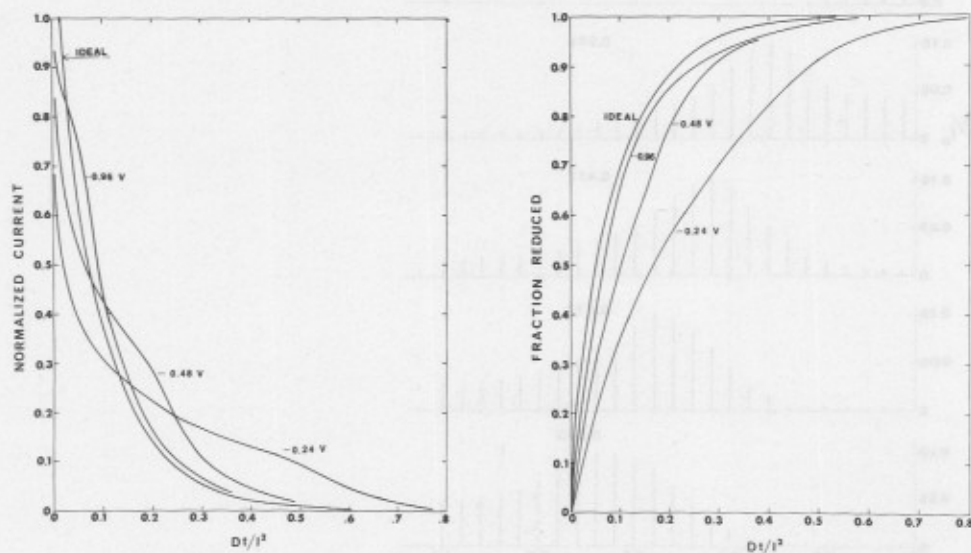

Fig. 8. Digital simulation of current–time and coulomb–time behavior during a potential step expt. for a system in which $\sigma_{ps} = 12.0$, at different values of applied potential, $E = E_{\frac{1}{2}} - x$ where x is shown next to each curve.

edge of the electrode nearest the reference electrode will be more negative. Hence, all other parts of the electrode will be more negative so that a greater portion of the electrode will be at the limiting current region. Simulations of this process for a system where $\sigma_{ps} = 12$ are shown in Fig. 8. This method, however, has its practical limits because currents due to double layer charging and secondary electrode processes can contribute to the total current. Recently, Tom and Hubbard[12] developed a thin layer cell which overcomes this iR problem by using a single electrode thin layer cell with a porous glass wall. Their method, however, cannot be applied to thin layer systems where transparency is a requirement or where the cell must be used in a restricted space, e.g., e.s.r. cells. Probst[13] has recently carried out some measurements of the iR drop across a thin layer cell which was designed to minimize edge effects and iR gradients. He found that both the uncompensated resistance, shown as R_u in Fig. 1, as well as the resistance of the thin layer of electrolyte, were significant. He also obtained a current–time curve similar to Fig. 5.

CONCLUSIONS

Simulations of processes in thin layer cells show the effect of resistance on both potential step and current step experiments. Without difficulty, these calculations may also be extended to include linear sweep voltammetry. Other electrochemical systems that exhibit non-uniform current densities due to iR drops include optical-electrochemical cells[2], cells with porous electrodes[3], and large scale electrochemical synthesis systems. Systems with optically transparent electrodes[14] such as used in optical reflectance measurements, have similar problems except that here the resistance is in the very thin electrode which is deposited on the glass wall[1]. Calculations may also be carried out for these types of systems. These results also suggest that thin layer cells will be very difficult to use with highly resistive nonaqueous solvents such as dimethylformamide or acetonitrile.

ACKNOWLEDGMENT

APPENDIX

I. Derivation of σ_{cs}

The voltage drop in a constant current experiment is given by $E = iR$. This potential difference can be converted to dimensionless units by multiplication of nF/RT, so that

$$\sigma_{cs} = (nF/\mathscr{R}T)iR \qquad (A-1)$$

Since the resistance of the solution measured across the length of the cell is $\rho L/lW$, the dimensionless parameter which describes the effect of internal resistance is

$$\sigma_{cs} = (nF/\mathscr{R}T)(\rho iL/lW) \qquad (A-2)$$

II. Derivation of σ_{ps}

The time dependence of the current in a potential step experiment where the final potential is on the plateau of the electrochemical wave is given by eqn. (A-3) (see eqn. (45) of ref. 1a)

$$i = \left(\frac{nFLWDc}{l}\right) 4 \sum_{m=1}^{\infty} \exp\left[\frac{-(2m-1)^2\pi^2 Dt}{l^2}\right] \tag{A-3}$$

If the term before the summation in eqn. (A-3) is substituted into an equation similar to eqn. (A-1), and the resistance $\rho L/lW$ is substituted for R, σ_{ps} becomes

$$\sigma_{ps} = (nF/\mathscr{R}T)(nFLWDc/l)(\rho L/lW)$$
$$\sigma_{ps} = (n^2 F^2/\mathscr{R}T)(\rho DcL^2/l^2) \tag{A-4}$$

SUMMARY

A digital simulation technique has been used to treat electrochemical reactions in thin layer electrochemical cells in which non-uniform current densities will result because of high electrolyte resistance. Calculations have been applied to chronopotentiometric, chronoamperometric, and chronocoulometric experiments. Current densities and potentials as a function of the electrode length are given for a variety of conditions.

REFERENCES

1 (a) A. T. Hubbard and F. C. Anson in A. J. Bard (Ed.), *Electroanalytical Chemistry, Vol. 4*, Marcel Dekker, New York, 1970.
   (b) C. N. Reilley, *Rev. Pure Appl. Chem.*, 18 (1967) 1221 and references therein.
2 R. W. Murray, W. R. Heineman and G. W. O'Dom, *Anal. Chem.*, 39 (1967) 1666.
3 R. de Levie in P. Delahay (Ed.), *Advances in Electrochemistry and Electrochemical Engineering. Vol. 6*, Interscience, New York, 1967.
4 (a) L. H. Piette, P. Ludwig and R. N. Adams, *Anal. Chem.*, 34 (1962) 916.
   (b) I. B. Goldberg and A. J. Bard, *J. Phys. Chem.*, 75 (1971) 3281.
5 I. B. Goldberg, A. J. Bard and S. W. Feldberg, submitted to *J. Phys. Chem.*
6 (a) J. Newman in A. J. Bard (Ed.), *Electroanalytical Chemistry, Vol. 6*, Marcel Dekker, New York, 1972, in press.
   (b) J. E. Harrar and I. Shain, *Anal. Chem.*, 38 (1966) 1148.
7 S. W. Feldberg in A. J. Bard (Ed.), *Electroanalytical Chemistry, Vol. 3*, Marcel Dekker, New York, 1969, and references therein.
8 K. B. Prater and A. J. Bard, *J. Electrochem. Soc.*, 117 (1970) 209, 335, 1517.
9 S. W. Feldberg in J. S. Mattson, H. P. Mark, Jr., H. C. MacDonald, Jr. (Eds.), *Applications of Computers to Chemical Instrumentation*, Marcel Dekker, New York, and references therein.
10 H. M. Lieberstein, *A Course in Numerical Analysis*, Harper and Row, New York, 1968, pp. 3, 6; A. Ralston, *A First Course in Numerical Analysis*, McGraw-Hill, New York, 1965, p. 495; R. W. Hamming, *Numerical Methods for Scientists and Engineers*, McGraw-Hill, New York, 1962, p. 352.
11 C. R. Christiansen and F. C. Anson, *Anal. Chem.*, 35 (1963) 205.
12 G. M. Tom and A. T. Hubbard, *Anal. Chem.*, 43 (1971) 671.
13 R. C. Probst, *Anal. Chem.*, 43 (1971) 994.
14 A. Yildiz, P. T. Kissinger and C. N. Reilley, *Anal. Chem.*, 40 (1968) 1018.